Fluorescence Method of Studying Void Closure Kinetics During Film Formation from High-T Latex Particles

ÖNDER PEKCAN, MURAT CANPOLAT

Department of Physics, Istanbul Technical University, 80626, Maslak, Istanbul, Turkey

Received 24 April 1996; accepted 28 February 1997

ABSTRACT: Void closure process due to viscous flow was studied during film formation from high-T latex particles. Steady-state fluorescence and photon transmission techniques were used to probe the evolution of optical clarity during film formation. The latex films were prepared from pyrene (P)-labeled poly(methyl methacrylate) particles and annealed in 10-min time intervals above glass transition temperature. Fluorescence intensity from P was measured after each annealing step. A relation for void closure time versus fluorescence intensity was derived, using the Vogel–Fulcher equation. Viscosity constant B was measured from the above relation and found to be as 11 $\times 10^3$ K. © 1997 John Wiley & Sons, Inc. J Appl Polym Sci **66:** 655–661, 1997

Key words: void closure; fluorescence; latex film viscous flow

INTRODUCTION

Film formation from a polymer latex is a complicated, multistage phenomenon and depends strongly on the characteristics of colloidal particles. In general, aqueous or non-aqueous dispersions of colloidal particles with glass transition temperature (T_g) above the drying temperature are named high-T latex dispersions, however aqueous dispersion of colloid particles with T_g below the drying temperature is called low-T latex dispersion. The term "latex film" normally refers to a film formed from low-T particles where the forces accompanying the evaporation of water are sufficient to compress and deform the particles into a transparent, void-free film.[1,2] However, high-T latex particles remain essentially discrete and undeformed during the drying process. Latex films can also be obtained by compression-molding of a dried latex powder composed of polymers such as polystyrene or poly(methyl methacrylate) (PMMA) that has T_g above room temperature. Film formation from these dispersions can occur in several stages. In both cases, stage I corresponds to the wet initial state. Evaporation of solvent leads to stage II, in which the particles form a close packed array; here, if the particles are soft, they are deformed to polyhedrons. Hard latex, however, stays undeformed at this stage. Annealing of low-T particles causes diffusion across particle–particle boundaries, which leads the film to a homogeneous, continuous material. In annealing of high-T latex systems, however, deformation of particles first leads to void closure and then, after the voids disappear, diffusion across particle–particle boundaries starts.[3,4] In other words, void-closure is the rate-limiting step for film formation from hard latex particles.[5]

Polymer latex is an important industrial product, and its film formation process has therefore been the subject of much theoretical and experimental attention. Over the last several years, it has become possible to observe latex film formation at the molecular level. Small-angle neutron scattering has been used to examine deuterated particles in a protonated matrix.[6] Alternatively, the process of interparticle polymer diffusion has been studied by direct nonradiative energy trans-

Correspondence to: Ö. Pekcan.

Journal of Applied Polymer Science, Vol. 66, 655–661 (1997)
 CCC 0021-8995/97/040655-07

fer (DET) using fluorescence decay measurements in conjunction with particles labeled with appropriate donor and acceptor chromophors.[7–9] This transient fluorescence technique has been used to examine latex film formation of 1-μm-diameter high-T (PMMA) particles[7] and of 100-nm-diameter low-T poly(butyl methacrylate) particles.[8,9] These studies all indicate that in the particular systems examined, annealing the films above T_g leads to polymer interdiffusion at the particle–particle junction as the particle interface heals. DET and the steady-state fluorescence technique have been used in this laboratory to study the interdiffusion process at the particle–particle junction during film formation from PMMA latex particles.[10–14] Recent investigations of latex film formation by using ultraviolet-visible (UVV) technique[15] in our laboratory have shown that particle coalescence can be distinguished in two different categories: first, the void closure process starts where molecularly contacting interfaces between particles can be established. Second, interdiffusion of chains takes place across the interface.

Determining the rate-limiting step during the film formation from a latex is of scientific interest, because it can provide insight into the mechanism of the process. It has been suggested that there are two important components in the process of latex film formation; the first is the evaporation of the solvent, and second is deformation of particles leading to void closure.[3,5] Equations were proposed to describe how the time for film formation varies as a function of the temperature of the latex, when each of the steps are rate-limiting.[5]

In this work, since non-aqueous, high-T latex dispersions are used, deformation of particles leading to void closure is believed to be the rate-limiting step for film formation. Here we studied the transparency evolution of films formed from high-T latex particles, by monitoring the scattered excited light (I_{sc}) and fluorescence emission intensity (I_{op}) from a dye using steady-state fluorescence (SSF) technique. Transmitted photon intensity (I_{tr}) was also monitored by UVV spectrophotometry during latex film formation. It was shown that the variation in transparency is related to the variation in I_{op} and I_{tr} intensities. Isothermal experiments were performed by annealing latex films in equal time intervals, and direct fluorescence emission was monitored to study viscous flow during film formation. Increase in I_{op} and I_{tr} intensities by increasing the number of annealing time intervals was attributed to the void-closure process. A relation was derived between void closure time and I_{op} intensity and used to interpret the time-dependence of fluorescence emission intensity during the void-closure process.

EXPERIMENTAL

In this work, high-T latex particles labeled with pyrene (P) dye and having two components were used[16,17]; the major part, PMMA, comprises 96 mol % of the material, and the minor component, polyisobutylene (PIB) (4 mol %), forms an interpenetrating network through the particle interior[18,19] very soluble in certain hydrocarbon media. A thin layer of PIB covers the particle surface and provides colloidal stability by stearic stabilization.

Films were prepared from the dispersion of particles by placing different numbers of drops on round silica window plates with a diameter of 1.35 cm and allowing the heptane to evaporate. Then samples were isothermally annealed above T_g of PMMA for 10-min time intervals at 150, 160, 170, 180, and 190°C temperatures. Details have been published elsewhere.[14] The temperature was maintained within $\pm 2°$ during annealing. After annealing, each sample was placed in the solid surface accessory of a Perkin–Elmer Model LS-50 fluorescence spectrometer. P was excited at 345 nm and fluorescence emission was detected between 370 and 440 nm. All measurements were carried out in the front-face position at room temperature. Slit widths were kept at 2.5 mm during all SSF measurements. UVV measurements were performed using a Shimadzu model 160A spectrophotometer between 300 and 400 nm.

Void Closure Kinetics

The void closure kinetics can determine the time for optical clarity and film formation.[5] An expression to relate the shrinkage of spherical void radius r to the viscosity of surrounding medium, η, was derived and is given by the following relation[4]:

$$\frac{dr}{dt} = -\frac{\gamma}{2\eta}\left(\frac{1}{\rho(r)}\right) \qquad (1)$$

where γ is the surface energy, t is time, and $\rho(r)$ is the relative density. It must be noted that here surface energy causes a decrease in void size and the term $\rho(r)$ varies with the microstructural

characteristics of the material, such as the number of voids, the initial particle size, and packing. Equation (1) is similar to one which was used to explain the time dependence of the minimum film-formation temperature during latex film formation.[20] If the viscosity is constant in time, integration of eq. (1) gives the relation as

$$t = -\frac{2\eta}{\gamma}\int_{r_0}^{r}\rho(r)\,dr \qquad (2)$$

where r_0 is the initial void radius at time $t = 0$.

The temperature dependence of viscosity of most amorphous polymers near their T_g can be described by the Vogel–Fulcher[21,22] equation as

$$\eta = A\exp\left(\frac{B}{T - T_0}\right) \qquad (3)$$

where A, B, and T_0 are the constants for a given polymer. For most glasses T_0 is typically about 50 K, lower than T_g. Combining eqs. (2) and (3), the following useful equation is obtained:

$$t = -\frac{2A}{\gamma}\exp\left(\frac{B}{T - T_0}\right)\int_{r_0}^{r}\rho(r)\,dr \qquad (4)$$

Equation (4) will be employed to interpret the fluorescence data to explain the void closure mechanism in the following sections.

RESULTS AND DISCUSSION

Optical Clarity and Path of Photons in Films

It has been shown[14,15] that when P-labeled latex films were annealed at a given temperature for increasing time intervals and excited at 345 nm, I_{op} and I_{tr} increased; however, I_{sc} was decreased continuously by increasing number of annealing time intervals. I_{op}, I_{sc}, and I_{tr} intensities versus annealing time are plotted in Figure 1(a–c), respectively, for the sample annealed at 180°C for 10-min time intervals. In order to interpret these behaviors of I_{op}, I_{sc}, and I_{tr} intensities, Monte Carlo simulations were performed to calculate the number of scattered (N_{sc}), transmitted (N_{tr}), and emitted (N_{Op}) pyrene photons from the latex film[14]; these are plotted against mean free path $\langle l\rangle$ of a photon in Figure 2(a–c), respectively. Here we note the similarities between Figures 1 and 2, from which one may suggest that as the annealing time increases, $\langle l\rangle$ of a photon increases due to void closure between particles in the latex film at the early stage of annealing in which both I_{op} and I_{tr} (N_{op} and N_{tr}) start to increase. Later, however, both I_{op} and I_{tr} (N_{op} and N_{tr}) saturate by increasing time and $\langle l\rangle$, respectively, by indicating that the void-closure process is completed.

This picture can be visualized by Frenkel's neck formation model,[23] which considers identical contacting spheres under the influence of surface

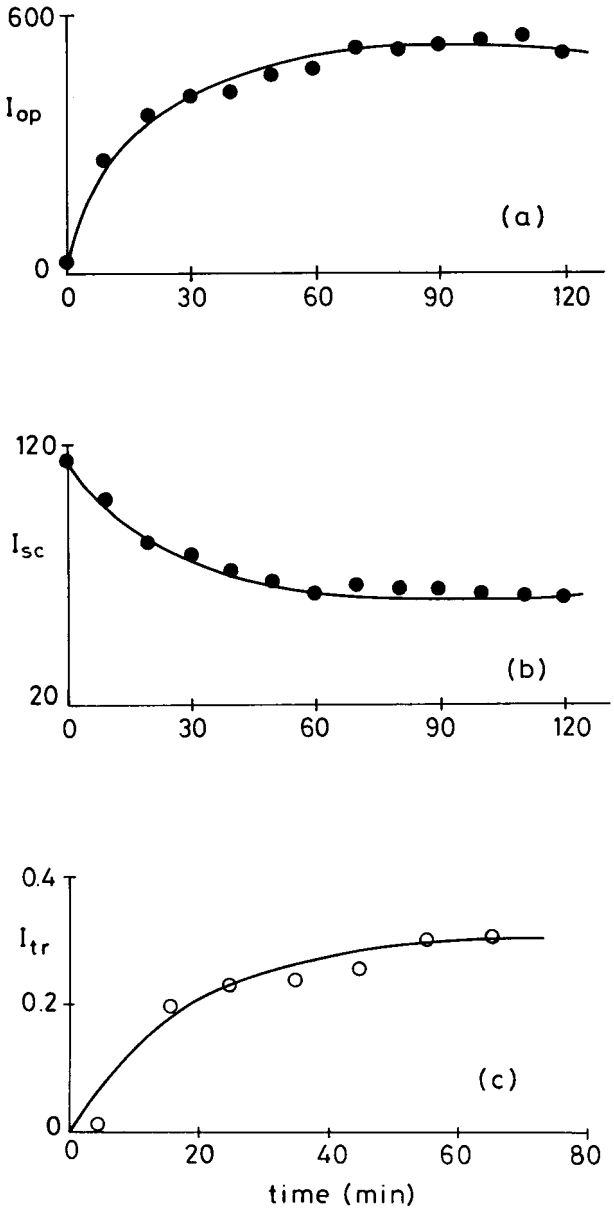

Figure 1 Plot of: (a) I_{op}, (b) I_{sc}, and (c) I_{tr} versus annealing time for film samples excited at 345 nm and annealed for 10-min time intervals.

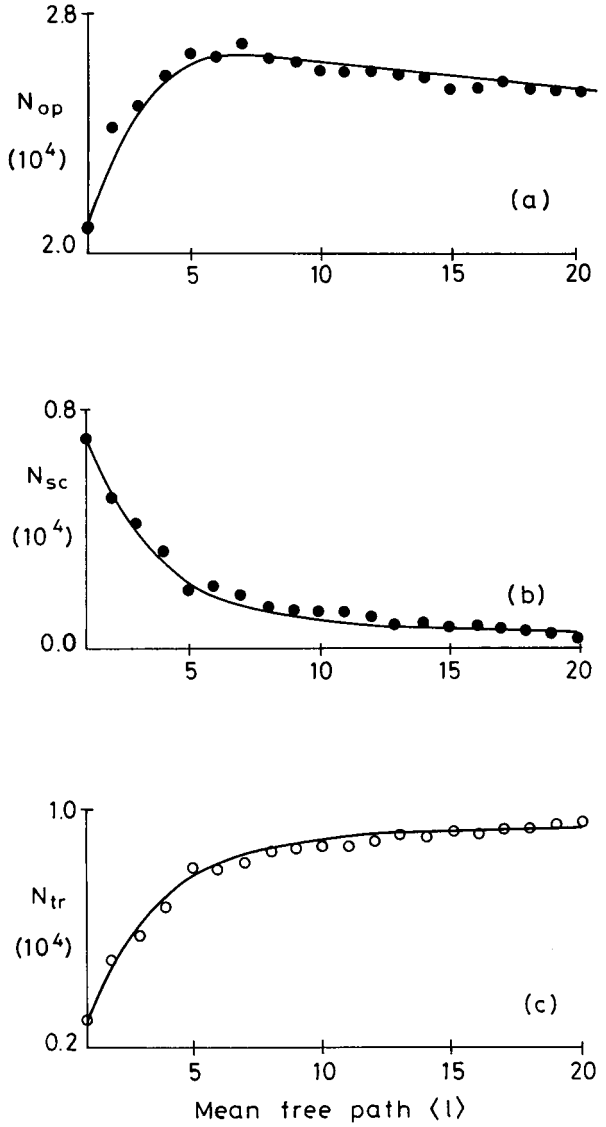

Figure 2 Variation in number of photons (a) emitted N_{op}, (b) scattered N_{sc}, and (c) transmitted N_{tr} from the front and back surfaces of a film with respect to mean free path $\langle l \rangle$ of a photon. Number of incident photons for each $\langle l \rangle$ is taken as 3×10^4 during Monte Carlo simulations.

tension. This model assumes that the displaced volume is redistributed uniformly such that the remaining surfaces keep their spherical shapes but with larger radii, which offers a longer mean free path, $\langle l \rangle$, of a photon during its journey in the latex film. Figure 3 illustrates Frenkel's picture for neck formation process from latex particles, where spherical voids are also presented before and after the neck growth.

The variations in I_{op} and N_{op} depend on the mean optical path, s, of a photon in the film. This mean optical path is directly proportional to the probability of the photon encountering a pyrene molecule. At the very early stage of annealing, the photon is scattered from the particle surfaces and the mean free path, $\langle l \rangle$, is of the order of the size of the particle and interparticle voids; after a few steps, the photon reemerges from the front surface of the film. Thus the mean optical path, s, is very short, which gives rise to high I_{sc} (and N_{sc}) and low I_{op} and I_{tr} (N_{op} and N_{tr}) values. As the viscous flow proceeds, some of the voids disappear and s becomes of the order of the deformed particle size. Clearly, in this stage, with the same number of rescattering, a photon will spend much longer time in the film; consequently, I_{op} (and N_{op}) increase whereas I_{sc} (and N_{sc}) decrease. The slight decrease in N_{op} at high $\langle l \rangle$ values in Figure 2(a) can be interpreted by the escape of some photons from the back surface of the film. Naturally, as $\langle l \rangle$ increases, photons can easily reach the back surface and N_{op} decrease whereas N_{tr} still increase [Fig. 2(c)].

In order to support these findings, scanning electron micrographs (SEM) of latex films before and after annealing at 160 and 180°C for a total of 30 min are presented in Figure 4. Figure 4(a) shows individual latex particles in powder film where many voids can be observed. However, in Figure 4(b,c), SEM images present the void-closure phenomenon due to annealing of latex films

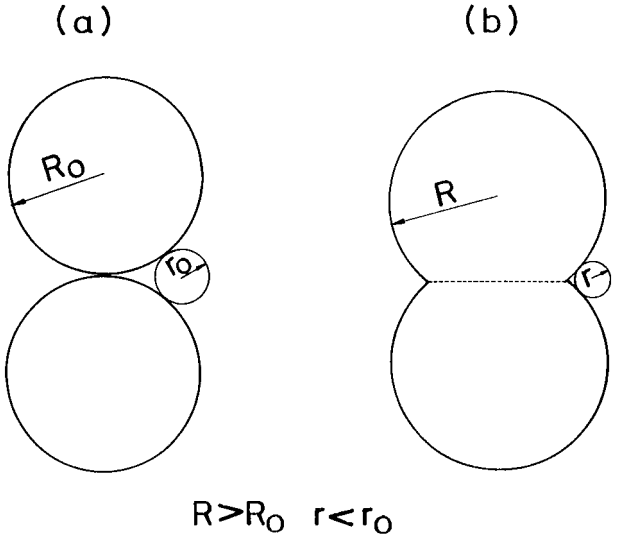

Figure 3 Geometrical representation of Frenkel's neck growth model between identical particles (a) before and (b) after neck growth. R_0,R and r_0,r are the particle and void radii before and after neck growth, respectively.

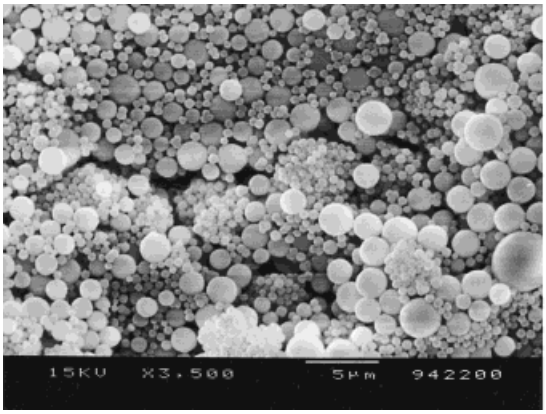

(a)

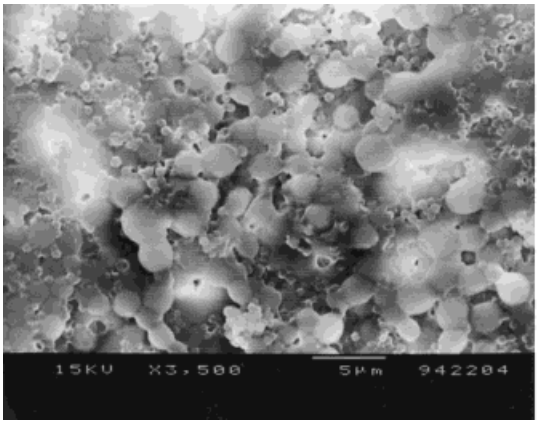

(b)

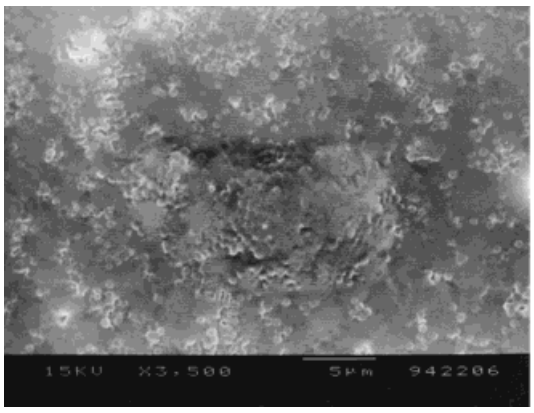

(c)

Figure 4 Scanning electron micrographs of latex film samples (a) before annealing, (b) annealed at 160°C for 2 × 10 min, and (c) annealed at 180°C for 2 × 10 min.

in 30 min total time at 160 and 180°C, respectively. The films in Figure 4(b,c) present higher I_{op} intensities than the film in Figure 4(a), indicating that photons have longer $\langle l \rangle$ and s values in the former samples, where refraction can occur many times between deformed particle interfaces.

SEM results, together with Monte Carlo simulations, support SSF and UVV observations in Figure 1. Cartoon representations of film formation from high-T latex particles and its relation with $\langle l \rangle$ and s are presented in Figure 5 for further illustration of our findings. Figure 5 presents the early stage of film formation, in which heptane evaporates and close-packed particles form a powder film that includes many voids. In this film $\langle l \rangle$ and s values are quite short and a photon is emitted immediately from the front surface of the film, which should have low I_{op} and I_{tr} but high I_{sc} values. Figure 5 represents a film where, due to annealing, void closure is completed and particles are deformed; as a result, incident photons have longer $\langle l \rangle$ values. In this case a photon can be refracted many times in the film and can have higher probability of finding a pyrene molecule. This film should emit high I_{op} and low I_{sc} intensities; however, higher I_{tr} can be obtained for these almost-transparent films.

Void Closure During Film Formation

When film samples were annealed at 150, 160, 170, 180, and 190°C for 10-min time intervals, a

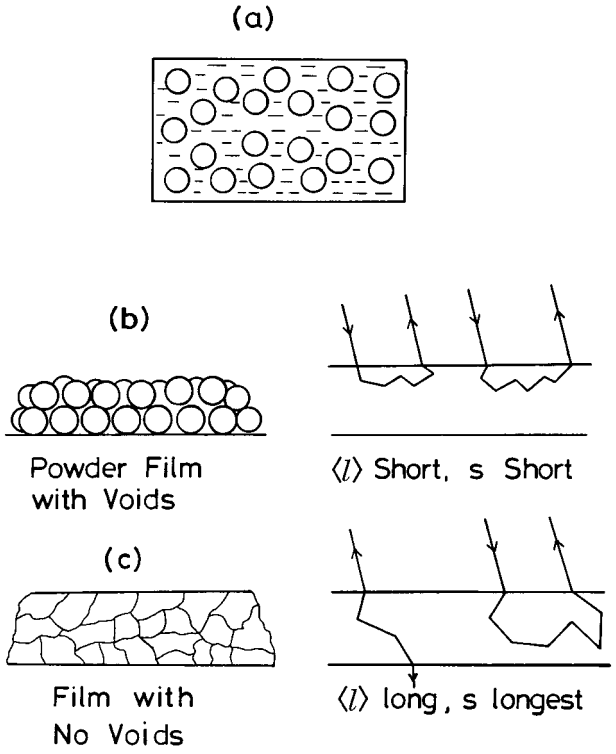

Figure 5 Cartoon representation of latex film formation stages. (a) Latex dispersion, (b) powder latex film, (c) film with no voids. $\langle l \rangle$ and s represent mean free and optical paths, respectively, of photon travel in the films.

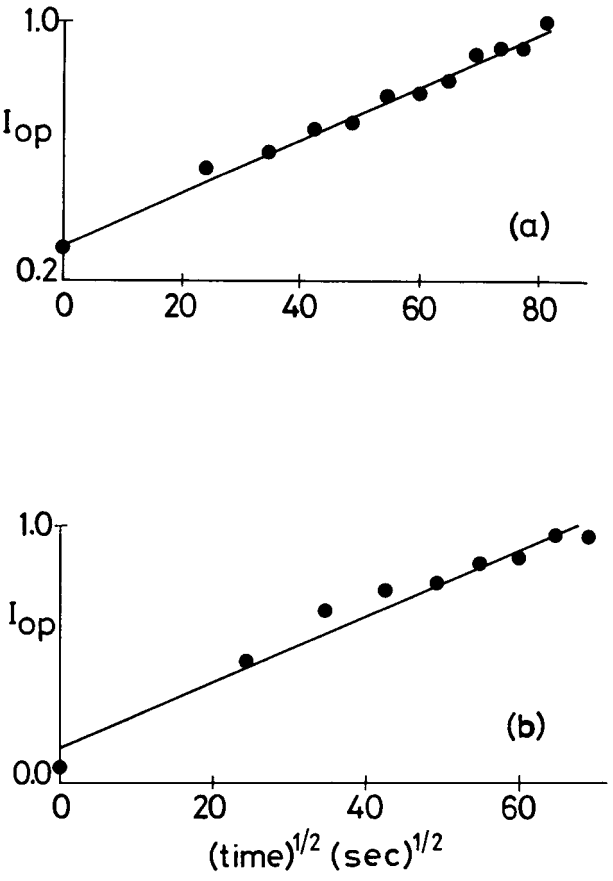

Figure 6 Plot of I_{op} versus $t^{1/2}$ for samples annealed at (a) 160°C and (b) 180°C in 10-min intervals.

continuous increase in I_{op} was observed until they were saturated. The increase in I_{op} was explained in the previous sections as resulting from an increase in optical clarity of latex film due to the disappearance of voids.

In order to quantify the above results, eq. (4) can be used where we assume that the voids are spherical (i.e., $\rho(r) \propto r^{-3}$). Integration of eq. (4) then produces the relation

$$t = \frac{2AC}{\gamma} \exp\left(\frac{B}{T - T_0}\right)\left(\frac{1}{r^2} - \frac{1}{r_0^2}\right) \qquad (5)$$

Here, C includes the related constants for the relative density, $\rho(r)$.

In the previous section it was stated that as void radius (r) decreases, the mean free path $\langle l \rangle$ of a photon increases, which then causes an increase in I_{op} intensity. Here an assumption can be made that I_{op} intensity is inversely proportional to void radius r. Then eq. (5) can be written as

$$t = \frac{2AC}{\gamma} \exp\left(\frac{B}{T - T_0}\right) I_{op}^2 \qquad (6)$$

where it is naturally considered that the initial radius of void, r_0, is larger than r, which then results in the omission of r_0^{-2} compared with r^{-2}. Equation (6) can be solved for I_{op} to interpret the experimental results as

$$I_{op} = S(T)t^{1/2} \qquad (7)$$

where

$$S(T) = \left(\frac{\gamma}{2AC}\right)^{1/2} \exp\left(\frac{B}{2(T - T_0)}\right) \qquad (8)$$

In Figure 6, I_{op} values are plotted against $t^{1/2}$ for films annealed at 160 and 180°C. I_{op} increases linearly for all samples, which indicates that the model chosen for void closure mechanism works well for our fluorescence data. The slopes in Figure 6(a,b) produce temperature-dependent parameter $S(T)$ which can also be plotted versus $(T - T_0)^{-1}$ to produce B values. The logarithmic plot of $S(T)$ versus $(T - T_0)^{-1}$ is shown in Figure 7, which also presents nice linear relation indicating that the void closure model used fits our data quite well. B is found to be 11×10^3 K, which is three times larger than the value obtained for an acrylic (4×10^3 K)[24] and 50 times larger than waterborne acrylic latices.[5,25] Especially in waterborne copolymer latices with very low T_g (270 K), strong plasticizing effect may cause very low B values. In that sense the measured value of B, in our case, strongly suggests that heptane has no

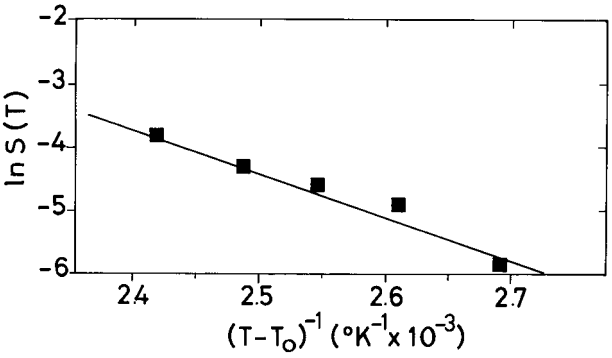

Figure 7 Logarithmic plot of $S(T)$ values versus $(T - T_0)^{-1}$ for the data obtained from Figure 6. Slopes were obtained by fitting the data to eq. (8), which produce B value as 11×10^3 °K.

plasticizing effect on PMMA latex particles, which is not surprising for annealed hard latex films well above T_g (380 K).

In conclusion, this work employed photon diffusion theory in conjunction with SEM to study the void-closure process during film formation from high-T latex particles. Here we have shown that a simple kinetic model for void closure is well fitted to our fluorescence data, which is also simple to produce.

The authors thank professor M. A. Winnik for supplying them with the latex material and stimulating them with his ideas.

REFERENCES

1. S. T. Eckersley and A. Rudin, *J. Coatings Technol.,* **62,** 89 (1990).
2. M. Joanicot, K. Wong, J. Maquet, Y. Chevalier, C. Pichot, C. Graillat, P. Linder, L. Rios, and B. Cabane, *Prog. Coll. Polym. Sci.,* **81,** 175 (1990).
3. P. R. Sperry, B. S. Snyder, M. L. O'Downd, and P. M. Lesko, *Langmuir,* **10,** 2619 (1994).
4. J. K. Mackenzie and R. Shutlewort, *Proc. Phys. Soc.,* **62,** 838 (1946).
5. J. L. Keddie, P. Meredith, R. A. L. Jones, and A. M. Ronald, *Proc. ACS,* Chicago, 1995.
6. K. D. Kim, L. H. Sperling, and A. Klein, *Macromolecules,* **26,** 4624 (1993).
7. Ö. Pekcan, M. A. Winnik, and M. D. Croucher, *Macromolecules,* **23,** 2673 (1990).
8. Y. Wang, C. L. Zhao, and M. A. Winnik, *J. Chem. Phys.,* **95,** 2143 (1991).
9. Y. Wang and M. A. Winnik, *Macromolecules,* **26,** 3147 (1993).
10. Ö. Pekcan, M. Canpolat, and A. Göçmen, *Polymer,* **34,** 3319 (1993).
11. M. Canpolat and Ö. Pekcan, *Polymer,* **36,** 2025 (1995).
12. Ö. Pekcan, *Trends Polym. Sci.,* **2,** 236 (1994).
13. Ö. Pekcan and M. Canpolat, *Polymers for Adv. Tech.,* **5,** 479 (1994).
14. M. Canpolat and Ö. Pekcan, *Polymer,* **36,** 4433 (1995).
15. Ö. Pekcan and F. Kemeroğlu, *J. App. Polym. Sci.,* submitted.
16. M. A. Winnik, M. H. Hua, B. Hongham, B. Williamson, and M. D. Croucher, *Macromolecules,* **17,** 262 (1984).
17. Ö. Pekcan, M. A. Winnik, and M. D. Croucher, *Macromolecules,* **17,** 262 (1994).
18. Ö. Pekcan, M. A. Winnik, and M. D. Croucher, *Phys. Rev. Lett.,* **61,** 641 (1988).
19. Ö. Pekcan, *Chem. Phys. Lett.,* **20,** 198 (1992).
20. G. B. Mc Kenna, in *Comprehensive Polymer Science, Vol. 2,* C. Booth and C. Price, Eds., Pergamon Press, Oxford, U.K., 1989.
21. H. Vogel, *Phys. Z.,* **22,** 645 (1925).
22. G. S. Fulcher, *J. Am. Ceram. Soc.,* **8,** 339 (1925).
23. J. Frenkel, *J. Phys. (USSR),* **9,** 385 (1945).
24. D. W. van Krevelen and P. J. Hoftyzer, *Properties of Polymer, Their Estimation and Correlation with Chemical Structure,* Elsevier, Amsterdam, 1976.
25. J. L. Keddie, P. Meredith, R. A. L. Jones, and A. M. Donald, *Macromolecules,* **28,** 2673 (1995).